Anisotropic Coherence properties in a trapped quasi2D dipolar gas

Christopher Ticknor

Theoretical Division, Los Alamos National Laboratory, Los Alamos, New Mexico 87545, USA

(Dated: October 3, 2012)

We consider a trapped quasi2D dipolar Bose Einstein condensate (q2D DBEC) with a polarization tilted into the plane of motion. We show that by tilting the polarization axis, the coherence properties are anisotropic. Such a system will have density fluctuations whose amplitude depend on their trap location. Additionally, interference contrast will also be anisotropic despite an isotropic density profile. The anisotropy is related to a roton like mode that becomes unstable and supports local collapse along the polarization axis.

Coherence properties underlie collective quantum behavior. An example of a need to further understand coherence is in high T_c superconductors [1], where the origin of the phase coherence leading to superconducting behavior is still mysterious. Such solid state systems where this occurs are complex, making the study of coherence properties a challenge. One avenue to study coherence of quantum systems more clearly is in ultracold gases, which have offered direct insight and unprecedented control to the study of quantum collective behavior. For example, two macroscopic Bose Einstein condensates (BECs) were interfered displaying phase coherence [2]. More refined experiments have directly detected higher order correlations [3] which cannot be easily accessed by electronic systems. Additionally, reduced dimensional ultracold gases have been the focus of intense interest because fluctuations are enhanced in such geometries. Phase coherence has been studied at the Berezinskii Kosterlitz Thouless (BKT) transition [4, 5] where two independent q2D ultracold gases were interfered, revealing thermally activated phase defects are the origin of decoherence [6]. The BKT transition is a transition where the phase coherence changes character, and insights into controlling such coherence properties are of general importance. In this paper we show the coherence properties of a trapped dipolar gas can be controlled.

The progress of experiments to probe ultracold gases is remarkable. Recent advances in imaging q2D ultracold gases have been used to detect density fluctuations [7–9]. Additionally, ultracold atomic systems in one dimensional systems have also amazingly been used to study quantum fluctuations directly [10] and other coherence properties [11–14]. For these examples of ultracold gases, the interaction between the constituents are short range. There are ultracold dipolar systems which have anisotropic, long range interactions, which offer an entirely new avenue to study quantum correlations and collective behavior. Amazing experimental progress has been made with the strongly magnetic atoms: Chromium (Cr), Dysprosium (Dy), and Erbium (Er). All three have been Bose condensed and displayed strong dipolar effects [15–17]. The study of dipoles in reduced geometries have begun with Cr, where it has been put into a one dimensional lattice, forming a series of coupled q2D dipolar BECs [18]. Additionally, polar molecules have been loaded into q2D geometries to control the rate of their chemical reaction [19].

Correlations of ultracold dipolar gases have been studied with a perpendicular polarization for weakly interacting gases near the roton instability [20–22] and strongly interacting gases, e.g. [23]. Using the direction of the polarization axis as a means to control the collective behavior and coherence properties, a q2D dipolar gas has been studied in the many body dipolar systems at the mean field level [24, 25] and for 2D dipolar scattering [26]. Additional theories have investigated a tilted polarization axis in a q2D dipolar fermi gas [27].

In this work, we go beyond mean field theory and examine the correlations of a trapped q2D DBEC at finite temperature with a partially tilted polarization into the plane of motion. This situation leads to anisotropic coherence properties, in which the gas maintains coherence along the direction of polarization, but more rapidly loses coherence perpendicular to the polarization direction. This anisotropy is evident in both the phase and density-density coherence properties. This emerges because of a roton-like mode in the excitation spectrum and is strongly anisotropic in character. We consider the implications of this theory through interference experiments and density fluctuations, both of which will exhibit anisotropic correlated behavior. We also calculate the compressibility of the dipolar gas.

To study the finite temperature coherence properties, we employ the Hartree Fock Bogoliubov method within the Popov approximation (HFBP) with nonlocal interactions [28, 29]. The HFB breaks the wavefunction into a condensate and thermal component: $\hat{\Psi} = [\sqrt{N_0}\phi_0(\vec{\rho}) + \hat{\theta}(\vec{\rho})]$ where we have replaced $\hat{a}_0 \rightarrow \sqrt{N_0}$. We use the Bogoliubov transformation: $\hat{\theta}(\vec{\rho}) = \sum_\gamma [u_\gamma(\vec{\rho})\hat{a}_\gamma e^{-i\omega_\gamma t} - v_\gamma^*(\vec{\rho})\hat{a}_\gamma^* e^{i\omega_\gamma t}]$ where $\hat{a}_\gamma$ ($\hat{a}_\gamma^*$) is the bosonic annihilation (creation) operator for the γth quasiparticle. The HFBP solves a non-local, generalized Gross-Pitaevskii equation and a nonlocal Bogoliubov de Gennes set of equations from which the eigenvalues and vectors (quasiparticles) are self-consistently obtained [29].

To evaluate the interaction, we assume a dipole moment of the form: $\vec{d} = d[\hat{x}\sin(\alpha) + \hat{z}\cos(\alpha)]$ where α

is the angle between $\hat{z}$ and $\hat{d}$, and we assume a single transverse Gaussian wavefunction of width l_z is occupied in the z direction, where $l_i = \sqrt{\hbar/\omega_i m}$ and ω_i is the trapping frequency. This requires $\mu, T \ll \hbar\omega_z$, and this leads to a simple form of the interaction. We use an isotropic trap (x, y) with $l_z/l_\rho = 0.15$ (ω_z/ω_ρ=44.4), and an interaction strength of $g_d = 0.025$ and $g = 0$, where $g_d = d^2/\sqrt{2\pi}l_z$ and $g = \sqrt{8\pi}a/l_z$ with a being the 3D s-wave scattering length ($a \ll l_z$). The polarization angle is set to $\alpha/\pi = 0.25$, this is beyond the critical angle. The critical angle is when the interaction is zero along the x axis, so $\sin(\alpha_c) = 1/\sqrt{3}$. For $\alpha > \alpha_c \sim 0.2\pi$ there is an attractive region to the interaction. This value of α is picked to optimize the collapse with respect to particle number. If it were steeper, the critical number would be less, and the depletion would not be large enough to observe the desired behavior. In addition, if α were smaller then roton the mode would require many more particles to collapse, and the collapses would be more 3D in nature. For $\alpha/\pi = 0.25$, the system is well described by the q2D formalism. For these parameters, the trapping potential for Dy [Er] is $(\omega_\rho, \omega_z)/2\pi$= (12,533) [(48,2133)] Hz. In a trapped ideal 2D gas, Bose condensation can occur [30], and the the critical temperature is at $T_C/\hbar\omega = \sqrt{6N}/\pi \sim 0.78\sqrt{N}$. This is for the pure 2D trapped gas, we only use it as a reference temperature. Throughout this paper we work in trap units. It is important to mention that the examples given here are weakly interacting; the HFBP method cannot accurately handle strongly interacting dipolar gases ($\mu < 10\hbar\omega_\rho$) [29]. This criteria is from the deviation of the Kohn mode, or slosh mode, from $1\hbar\omega_\rho$. If the interaction is too strong then the static thermal cloud alters the slosh mode of the condensate; this is a numerical signature that the HFBP has broken down. This restricted the work from entering the Thomas Fermi regime where $l_\rho > \xi$, where ξ is the healing length ($\sqrt{m\mu/\hbar^2}$). Because of this, trapping effects are always important in this study.

Once g_d, g, l_z, T, α and the condensate number, N_0, are selected, the HFBP calculation finds: the number of thermal atoms, $\tilde{N}$; the chemical potential, μ; the condensate wavefunction, ϕ_0; and the quasiparticle wavefunctions, u_γ and v_γ. From these wavefunctions, we construct the correlation functions: the nonlocal thermal correlation function, $\tilde{n}(\vec{\rho}, \vec{\rho}') = \sum_\gamma [u_\gamma^*(\vec{\rho})u_\gamma(\vec{\rho}') + v_\gamma^*(\vec{\rho})v_\gamma(\vec{\rho}')]N_\gamma + v_\gamma^*(\vec{\rho})v_\gamma(\vec{\rho}')$ with N_γ being the Bose-Einstein occupation, and the condensate correlation function, $n_0(\vec{\rho}, \vec{\rho}')$, given by $N_0\phi_0^*(x)\phi_0(x')$. The total local density is $n(\vec{\rho}) = n_0(\vec{\rho}) + \tilde{n}(\vec{\rho})$ where e.g. $n_0(\vec{\rho}) = n_0(\vec{\rho}, \vec{\rho})$. The HFBP method uses these correlation functions in the self-consistent calculation, and they can be related to the more common g_1 and g_2 correlation functions [31]:

$$g_1(\vec{\rho}; \vec{\rho}') = \frac{\langle \Psi^*(\vec{\rho})\Psi(\vec{\rho}') \rangle}{\sqrt{n(\vec{\rho})n(\vec{\rho}')}} = \frac{n_0(\vec{\rho}, \vec{\rho}') + \tilde{n}(\vec{\rho}, \vec{\rho}')}{\sqrt{n(\vec{\rho})n(\vec{\rho}')}}, \quad (1)$$

$$g_2(\vec{\rho}; \vec{\rho}') = \frac{\langle \Psi^*(\vec{\rho})\Psi^*(\vec{\rho}')\Psi(\vec{\rho})\Psi(\vec{\rho}') \rangle}{n(\vec{\rho})n(\vec{\rho}')} \quad (2)$$

$$= 1 + g_1(\vec{\rho}, \vec{\rho}')^2 - \frac{n_0(\vec{\rho}, \vec{\rho}')^2}{n(\vec{\rho})n(\vec{\rho}')}.$$

g_1 details phase correlations, for example it determines the fringe contrast if a BEC were split and interfered. g_2 is the density-density correlation function, and is related to density fluctuations and the static structure factor [32].

We study a system with a temperature of $T/T_C = 0.5$. At this temperature, the condensate fraction is $N_0/N > 0.57$ for all N considered. This is well within the region of validity for the HFBP. This temperature thermally populates the quasiparticles, so that the anisotropy in the coherence properties is significant. Furthermore, this temperature makes the density more isotropic. Values of T/T_C between 0.4 and 0.6 produces similar results. Raising the temperature would lead to populating more thermal modes, and would make correlations isotropic, reflecting the nature of the trap ($T/T_C \sim 1$). For lower temperatures, the correlations are determined by the condensate's properties alone, as the depletion and thermal population become negligible. A pure condensate has total phase coherence, it is the thermal fraction that leads to reduced coherence.

We now look at the correlation functions, $g_1(\vec{\rho}; 0)$ and $g_2(\vec{\rho}; 0)$. These quantify the coherence of the system from the origin to $\vec{\rho}$. To illustrate the anisotropic coherence of the gas, we plot them along the polarization axis and in the perpendicular direction in figure 1.

Fig. 1 (a) shows the total density and Fig. 1 (b) shows $g_1(\vec{\rho}; 0)$ along the x (solid line) and y (dashed) axes. The important feature is that g_1 quickly decreases in the y direction, but only steadily decreases its value in the x direction or polarization direction. We have shown the system for three different number of total particles 2000 (blue), 3000 (red), and 4000 (black), from top to bottom at the temperature $T/T_C = 0.5$. Varying the number is like varying the interaction strength. The density is isotropic near the center of the trap, even when the g_1 is anisotropic. Near the edge of the trap the total density becomes anisotropic and is more extended in the x axis.

A recent Bragg spectroscopy experiment observed an anisotropic speed of sound for a 3D dipolar gas [33]. A similar experiment for a q2D DBEC could be used to probe these predicted anisotropic coherence properties. If a DBEC were split into two equal clouds such that one is moved by $\vec{a}$ with a relative phase of $S(\vec{\rho})$, then the total density would be $n(\vec{\rho}) = 0.5(n(\vec{\rho}) + n(\vec{\rho} + a)) + \sqrt{n(\vec{\rho})n(\vec{\rho} + \vec{a})}g_1(\vec{\rho}, \vec{\rho} + \vec{a})\cos[S(\vec{\rho})]$. The fringe contrast will depend on the angle between $\vec{a}$ and $\vec{d}$ because of the anisotropy in $g_1(\vec{\rho}, \vec{\rho} + \vec{a})$. To maximize the difference in
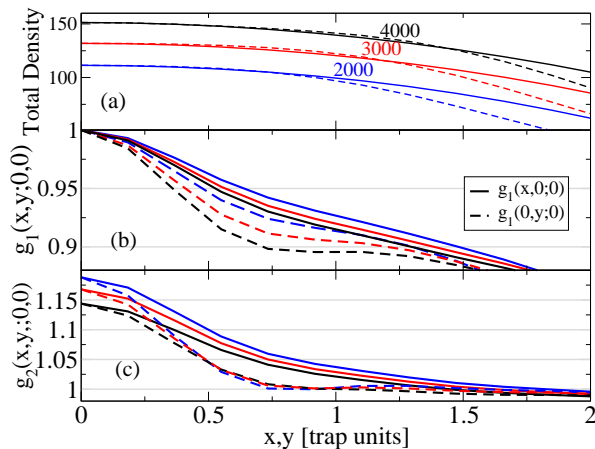
FIG. 1: (a) The total density, (b) $g_1(x,0;0,0)$ (solid line) and $g_1(0,y;0,0)$ (dashed), and (c) $g_2(x,0;0,0)$ (solid line) and $g_2(0,y;0,0)$ (dashed) at T/T_C=0.50 and for N =2000 (blue), 3000 (red), and 4000 (black) from top to bottom. The total density is isotropic in the center and yet the correlation function is significantly anisotropic at short range.

fringe contrast, the phase difference should be $\pi/2$ when $\vec{a}$ is near $3/4$ l_ρ. This signal is only a few percent and would be challenging to measure.

We now move on to the density-density correlation function, $g_2(\vec{\rho};0)$. In Fig. 1 (c), g_2 this is plotted along the x (solid line) and y (dashed) axis. The results are similar to those of g_1, the extent of the coherence is further in the x direction than the y. The anisotropy is more significant in this correlation function. The fact that the g_2 goes below one is a trap effect and is most significant when correlating with the trap center [11, 12]. This correlation function is important for density fluctuations, this will be discussed below.

To understand the nature of the anisotropy we look at the Bogoliubov de Gennes excitation spectrum as a function of particle number, this is shown in Fig. 2 (a). The spectrum goes soft or an eigenvalue becomes complex implying the system is unstable when there are more than 4850 particles. Additionally, we show contour plots of the wavefunctions of the two modes which go soft (u_γ) in Fig. 2 (b,c), and the dashed black lines are $\sqrt{n_0}$. The contours at 0.25, 0.5, and 0.75 of the maximum values of the individual wavefunctions, and for u_γ the shaded regions signify a region less than zero. These quasiparticle modes start with an energy at or above $4\hbar\omega_\rho$. Then as the particle number is increased, their energy decreases. In a homogeneous q2D DBEC, the roton is a local minimum in the excitation spectrum, which occurs near the $k_\rho l_z \sim 1$ [34]. If the spectrum goes soft, the system locally collapses into plane waves which form dense stripes along the polarization axis.

The Bogoliubov de Gennes excitation spectrum has been analyzed in detail in Ref. [29] for a dipolar gas with $\alpha = 0$ or a cylindrically symmetric system. In that

case there are degenerate modes with azimuthal symmetry $\pm m$. In the present case this degeneracy has been broken by the tilted polarization axis, leading to slightly different energies depending on the excitation shape relative to the x axis. This leads to band like structures forming in Fig. 2 (a).

The mode in 2 (b) makes a significant contribution to the correlation function for two reasons: first, it is a low energy mode, and is more thermally populated. Second, the correlation function, $g_i(\vec{\rho}:0)$, has a factor of $u_\gamma(0)$ and $v_\gamma(0)$ in it. Only a few low energy modes have a significant contribution at the origin. The breathing mode just below $2\hbar\omega$ and the roton mode in 2 (b) are two low energy modes with a maximum in the center of the trap. Other low energy modes have small or zero amplitude in the center of the cloud because symmetry.

In the trapped case, the finite extent of the gas alters the nature of the "roton" mode [35–37]. For $\alpha = 0$, the gas become 3D in nature, $\mu \sim \hbar\omega_z$ [22]. When the gas becomes unstable, it locally collapses and forms regions of high density. A good demonstration of this is given in Ref. [38]. For $\alpha/\pi \sim 0.25$, the stability of the system displays an interplay of the interaction and the trap geometry, while maintaining $\mu \ll \hbar\omega_z$. The collapse is local and forms a series density regions parallel to the polarization. In Fig. 2 (b,c), we see this character in the quasiparticles, which have an extended amplitude along the polarization axis and a series of nodes in the perpendicular direction. It is this character of the quasiparticles that leads to anisotropic character to the correlations. The nodes in the roton modes lead to destructive interference and reduce correlation in that direction.

To further study the implications of the anisotropic correlations, we consider the density fluctuations of the gas by calculating the compressibility: $kT\kappa(\vec{\rho}) = \langle \int d\vec{\rho}' \delta n(\vec{\rho}) \delta n(\vec{\rho}') \rangle = \int d\vec{\rho}' n(\vec{\rho}) n(\vec{\rho}') g_2(\vec{\rho};\vec{\rho}') - n(\vec{\rho})(N-1)$ where $\delta n(\vec{\rho}) = \hat{\Psi}^*(\vec{\rho})\hat{\Psi}(\vec{\rho}) - n(\vec{\rho})$ and this is the density fluctuations of the system. The compressibility and number fluctuations have been measured in BEC experiments [8, 9]. We present the compressibility for a trapped dipolar gas in Fig. 3 (b) at $T/T_0 = 0.5$ for 2000 (blue), 3000 (red), and 4000 (black) in the x (solid) and y (dashed). These results show that the density fluctuations roughly follow the anisotropic density profile. Another way to state this is: that depending on the local value of the density, the compressibility is determined almost uniquely.

In this work, we found that the correlations are anisotropic in a q2D DBEC with a polarization axis tilted into the plane of motion. We studied the DBEC with the HFBP at at temperature of $T/T_C \sim 0.5$. At this temperature, quasiparticles are thermally populated and total density is nearly isotropic in the central region of the trap. We computed the $g_1(\vec{\rho};0)$ and $g_2(\vec{\rho};0)$ correlations functions, which have anisotropic character in the center of the gas even though the density is isotropic in the central region of the DBEC. This has measurable implications for interference properties and density fluctuations of the gas. We found that the anisotropic correlations
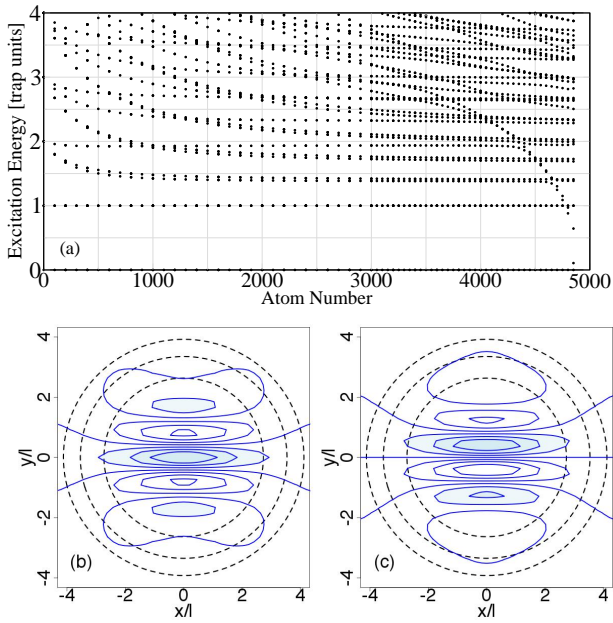
FIG. 2: (a) The Bogoliubov de Gennes spectrum is shown as a function of particle number for $g_d = 0.025$ for $\alpha/\pi = 0.25$. (b,c) A contour plot of the roton quasiparticle modes (u_γ) which go soft for a dipolar system with tilted polarization axis are also shown. The dashed black line is $\sqrt{n_0}$ and for u_γ the shaded regions are less than zero. The contours at 0.25, 0.5, and 0.75 the maximum values of the individual wavefunctions.
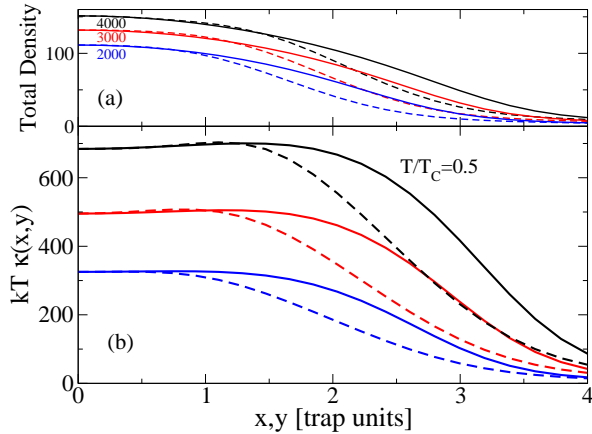

FIG. 3: (a) The total density (b) the compressibility, $kT\kappa(\vec{\rho})$, for the dipolar gas along the x (solid) and y (dashed) axis for particles number 2000 (blue), 3000 (red), and 4000 (black).

occur due to roton like quasiparticle modes that can lead to local collapse along the polarization axis.

An immediate extension of this work is to study the static structure factor such as was recently done in Ref. [22] at zero temperature. An important difference is that the static structure will become anisotropic, i.e. $S(k_x, k_y)$, and with present methods, it could be done at finite temperature [41]. This also presents a promising method to observe the anisotropic coherences predicted here.

Future work will be to investigate the impact of correlations at higher temperatures and strongly interactions where they might impact the BKT transition [4, 5, 39]. This will require an improvement to the method [40] or new approach altogether. Either way, it will be intriguing to study the impact of the anisotropic dipolar interaction on vortex correlations near the BKT transition and the time dependence of such a gas. The present work was not able to measure the decay of the correlation functions due to the relatively weak interaction strength or small number the numerical method could handle. If the next method can probe stronger interactions, we would hope to observe a different character in the decay of the correlation functions along and perpendicular to the polarization axis.

[1] T. Timusk and B. Statt, Rep. Prog. Phys. **62**, 61 (1999); V. M. Loktev, R. M. Quick, S. G. Sharapov, Physics Reports, **349**, 1 (2001).

[2] M. R. Andrews *et al.*, Science **275**, 553 (1997).

[3] For example: A. Ottl *et al.*, Phys. Rev. Lett. **95** 090404 (2005); S. S. Hodgman *et al.*, Science **331**, 1046 (2011); S. Foelling *et al.*, Nature **434**, 481 (2005).

[4] Berezinskii, V. L. Sov. Phys. JETP **34**, 610 (1972). L. M. Kosterlitz, D. J. Thouless, J. Phys. C **6**, 1181 (1973);

[5] Z. Hadzibabic and J. Dalibard, Riv. Nuo. Cime., **34**, 389 (2011).

[6] Z. Hadzibabic *et al.*, Nature **441**, 1118 (2006).

[7] T. Yefsah *et al.*, Phys. Rev. Lett. **107**, 130401 (2011).

[8] C.L. Hung *et al.*, Nature **470**, 236 (2011); N. Gemelke *et*

al., Nature **460**, 995 (2009).

[9] S. Tung *et al.,* Phys. Rev. Lett. **105**, 230408 (2010).

[10] J. Armijo, Phys. Rev. Lett. **108**, 225306 (2012).

[11] S. Manz *et al.*, Phys. Rev. A **81**, 031610 (2010).

[12] A. Imambekov *et al.*, Phys. Rev. A **80**, 033612 (2009).

[13] T. Kinoshita, T. Wenger, and D. S. Weiss, Phys. Rev. Lett. **95**, 190406 (2005).

[14] J. Armijo *et al.*, Phys. Rev. Lett. **105**, 230402 (2010).

[15] Th. Lahaye *et al.*, Nature **448**, 672 (2007); Th. Lahaye *et al.*, Nature Physics **4,** 218 (2008); Th. Lahaye *et al.*, Phys. Rev. Lett 101, 080401 (2008).

[16] K. Aikawa *et al.,* Phys. Rev. Lett. **108**, 210401 (2012).

[17] M. Lu *et al.,*, Phys. Rev. Lett., **107**, 109401 (2011); M. Lu *et al.,*, Phys. Rev. Lett., **108**, 215301 (2012).

[18] S. Meuller *et al.*, Phys. Rev. A **84**, 053601 (2011).

[19] M. H. G. de Miranda *et al.,* Nat. Phys. **7**, 502 (2010).

[20] M. Klawunn *et al.* Phys. Rev. A **84**, 033612 (2012).

[21] A. Sykes and C. Ticknor, arXiv1205.1350.

[22] P. B. Blakie, D. Baillie, and R. N. Bisset, Phys Rev. A, **86** 021604(R) (2012).

[23] H. P. Buechler *et al.*, Phys Rev Lett **98**, 060404 (2007);G. E. Astrakharchick *et al.*, Phys Rev Lett **98**, 060405 (2007).

[24] R. Nath, P. Pedri, and L. Santos, Phys. Rev. Lett. **102** 050401 (2009).

[25] C. Ticknor, R. M. Wilson, J. L. Bohn, Phys. Rev. Lett. **106**, 065301 (2011).

[26] C. Ticknor, Phys. Rev A **84**, 032702 (2011).

[27] M. M. Parish and F. M. Marchetti, Phys. Rev. Lett. **108**, 145304 (2012); L. M. Sieberer and M. A. Baranov, Phys. Rev. A **84**, 063633 (2012).

[28] A. Griffin, Phys. Rev. B, **53**, 9341 (1996).

[29] C. Ticknor, Phys. Rev. A **85**, 033629 (2012).

[30] V. Bagnato and D. Kleppner, Phys. Rev. A **44**, 7439 (1991).

[31] M. Naraschewski and R. J. Glauber, Phys. Rev. A **59**, 4595 (1999).

[32] F. Zambelli *et al.,* Phys. Rev. A **61** 063608 (2000).

[33] G. Bismut *et al.*, arXiv 1205.6305.

[34] L. Santos, G. V. Shlyapnikov, and M. Lewenstein, Phys. Rev. Lett. **90**, 250403 (2003).

[35] S. Ronen, D. C. E. Bortolotti, and J. L. Bohn, Phys. Rev. Lett. **98**, 030406 (2007).

[36] R. Wilson, S. Ronen, and J.L. Bohn Phys. Rev. Lett. **104**, 094501 (2010).

[37] R. M. Wilson, S. Ronen, and J. L. Bohn, Phys. Rev. Lett. **100**, 245302 (2008).

[38] N. G. Parker *et al.* Phys. Rev. A **79**, 013617 (2009).

[39] A. Filinov *et al.* Phys. Rev. Lett. **105**, 070401 (2010).

[40] C. Mora and Y. Castin, Phys. Rev. A **67**, 053615 (2003).

[41] A. Csordas, R. Graham, and P. Szepfalusy, Phys. Rev. A **54**, R2543 (1996).